

Effect of Coordinate Rotation Systems on Calculated Fluxes over a Forest in Complex Terrain: A Comprehensive Comparison

Takanori Shimizu¹

Received: 3 July 2013 / Accepted: 7 April 2015 / Published online: 29 April 2015
© Springer Science+Business Media Dordrecht 2015

Abstract Seven coordinate rotation systems were compared to determine a suitable system for a forest in complex terrain, using eddy-covariance data for a period of 40 days. The traditional double rotation was set as the standard of comparison with six other fixed coordinate systems, whose coefficients were carefully determined based on wind component data for a two-year period. Differences in total heat fluxes and daytime CO₂ fluxes calculated from all systems were small, except those from the sector-wise planar fit, which linearly and systematically underestimated the fluxes by about 5%. The nighttime CO₂ flux was also underestimated by the sector-wise planar fit, but there was significant scatter in the plots, and the mean difference was 7%. The standard deviations of the wind components and scalars normalized by the friction velocity and the dynamic parameters were calculated for each system, and the errors from the relationships obtained previously from flat and homogenous terrain were examined. The nighttime normalized standard deviation for scalars agreed better with the relationships after applying the sector-wise planar fit than those calculated by the other systems, although no remarkable difference was found in the daytime data. Therefore, the sector-wise planar fit was not the first choice for our site during daytime based on the energy imbalance, which was mainly caused by underestimating daytime heat fluxes. Double rotation or one of the four systems without the roll rotation process might be superior at our site. However, the offset error in the vertical wind component of the sonic anemometer induced errors of several percent in the fluxes in these systems, which was equivalent to the underestimation using the sector-wise planar fit. Meanwhile, the sector-wise planar fit system might still be the best system for calculating nighttime flux, considering the tendency of the nighttime normalized standard deviations.

Keywords Complex terrain · Coordinate system · Heat and mass fluxes · Offset error

✉ Takanori Shimizu
simizuta@affrc.go.jp

¹ Department of Soil and Water Conservation, Forestry and Forest Products Research Institute, 1 Matsunosato, Tsukuba, Ibaraki 305-8687, Japan

1 Introduction

Heat and tracer-gas (such as H₂O and CO₂) fluxes are now measured worldwide, using sonic anemo-thermometers with gas analyzers. Research has been extended to various ecosystems, including non-ideal terrain (Lee et al. 2004). Coordinate rotation of three-dimensional wind velocity components is one of the most significant processes in flux calculations. Coordinate rotation has helped interpret fluxes acquired over complex terrain, at least since McMillen (1988). His system is called the “triple rotation”, in which roll rotation is executed for $\overline{v'_r w'_r} = 0$ after yaw and pitch (or horizontal and vertical) rotations, to achieve $\overline{v_r} = \overline{w_r} = 0$. Here, v and w are lateral and vertical velocity components of the main flow vector (u), subscript r is the rotated component, and the overbar and prime denote the mean and fluctuation over a certain averaging time. To attain $\overline{w_r} = 0$, the mean vertical angle for the sonic anemo-thermometer ($= \tan^{-1}(\overline{w_s}/\overline{U_s})$, in which $\overline{U_s} = (\overline{u_s^2} + \overline{v_s^2})^{1/2}$ and subscript s is the wind-speed component obtained from the sonic anemo-thermometer, the same as “angle of attack” in Nakai et al. 2006), is applied as the pitch angle in the “double rotation” and triple rotation. The effectiveness of the final roll rotation for an actual complex flow has been suspect (e.g. Kaimal 1988; Finnigan 2004), and the double rotation was the most used coordinate rotation approach until a decade ago (e.g. Aubinet et al. 2000). However, applying double rotation or triple rotation occasionally leads to an over-rotation error in weak winds, when $\overline{w_s}$, the average vertical wind-speed component measured by the sonic anemo-thermometer, is large relative to the average horizontal components ($= \overline{U_s}$). This error, which is produced by an unrealistically large rotation angle, becomes more significant if w_s includes an instrumental offset error.

Wilczak et al. (2001) elaborated a coordinate system based on three-dimensional wind velocity components along the sonic anemo-thermometer orthogonal axes, obtained over a period of weeks or longer. This system is called the planar fit. In the system, vertical fluxes are along the normal vector of the fitting planar, which is determined by $\overline{u_s}$, $\overline{v_s}$, and $\overline{w_s}$ obtained during a period, via the least-squares method,

$$\overline{w_s} = a_{p0} + a_{p1}\overline{u_s} + a_{p2}\overline{v_s}, \quad (1)$$

where a_{p0} , a_{p1} , and a_{p2} are regression coefficients. These coefficients regulate the rotated plane, and the wind component vertical to the plane (w_r on the planar) is used for calculating the vertical fluxes. The planar fit removes over-rotation error from the fluxes, partly because it is a fixed system and the rotation angle is unaffected by temporal wind conditions, and partly because a_{p0} in Eq. 1, which includes the w_s offset error if it is constant, is eliminated from the flux calculation. Thus, the planar fit has been tested in many studies and has been proven a more stable system for estimating fluxes than that of double rotation (e.g. Turnipseed et al. 2003; Göckede et al. 2008). The single fitting planar was adopted, as the planar fit was originally developed for the sonic anemo-thermometer tilt correction. Meanwhile, the characteristics of flow distortion due to complex terrain and/or by instruments and attachments may depend on flow direction; thus, it is reasonable that the single planar may be inadequate for correcting such effects. The approach of Sun (2007), which was aimed at the appropriate interpretation of nighttime vertical advection from multiple sonic anemo-thermometer data, had a similar issue. Some coordinate systems have been proposed on the assumption that non-advective vertical flow should reflect the slope gradient around the observation site. However, it is difficult to define such a gradient value over very complex terrain with undulations and various slope angles.

This situation has motivated the development of other fixed coordinate rotation systems. Several fitting planes based on the planar fit concept have been applied to various wind

direction sectors, corresponding to terrain (e.g. Yuan et al. 2007; Mildenerger et al. 2009; Siebicke et al. 2012) or instrumental (e.g. Ono et al. 2008; Li et al. 2013) effects on airflow from each direction. The system was first proposed by Paw et al. (2000) and was called the “sector (-wise) planar fit” by Yuan et al. (2011) and Siebicke et al. (2012). This system makes it possible to avoid the offset error effect from the estimated flux values, as does the planar fit, although the offset value a_{p0} in Eq. 1 of each sector plane differs from the others. Furthermore, Siebicke et al. (2012) suggested that the sector-wise planar fit could make \bar{w}_r nearly zero for all wind directions and was more suitable for estimating nighttime CO₂ flux than the planar fit. In addition, this system seems conceptually acceptable and is analogous to a schematic concept of airflow over a complex terrain (e.g. Fig. 1 in Finnigan et al. 2003 and in Finnigan 2004). Therefore, this system has been recognized as the best method for complex terrain. However, an issue with the sector-wise planar fit may be that it often reduces flux values over complex terrain (e.g. Yuan et al. 2011).

Besides systems based on the planar fit, some fixed coordinate systems have been proposed. Lee (1998), Su et al. (2004), Vickers and Mahrt (2006), Kosugi et al. (2007), and Shimizu (2007) determined pitch rotation (or tilt) angle from a function involving wind direction and the ensemble average of the mean vertical angle at the sonic anemo-thermometer ($\tan^{-1}(\bar{w}_s/\bar{U}_s)$). However, applying an average vertical angle to estimate pitch rotation angle in a coordinate system potentially causes the instrumental offset error (e.g. Lee et al. 2004) to persist in the calculated fluxes.

Although there are uncertainties in each coordinate system, the effect of these systems on flux values has not been comprehensively examined. This is particularly true for complex terrain, where the choice of coordinate system may be more important than in flat topography. Whether fluxes calculated in complex terrain with a particular coordinate system are comparable to those calculated with another method has not been established. Accordingly, the objective of this study was to examine the effect of coordinate rotation systems on flux estimates over a forest in complex terrain. Using data from an AsiaFlux observation site in Japan, we compared momentum, heat, and CO₂ fluxes calculated using each coordinate system. Furthermore, we examined the agreement between the standard deviations of wind components (w_r and u_r) by friction velocity (σ_{wr}/u_* and σ_{ur}/u_* , respectively) or those of scalars (e.g. σ_T , where T is air temperature) over their dynamic parameters (e.g. dynamic temperature $T_* = \bar{w}_r T'/u_*$) with equations obtained previously (see Foken 2008a). We also discuss the effects of dataset length for setting fixed coordinate systems, and the vertical wind offset error in the methods (except the planar fit and sector-wise planar fit) on calculated fluxes.

2 Materials and Methods

Observations were made at the Kahoku Experimental Watershed (KHEW; 33°08'N, 130°43'E), one of the AsiaFlux network sites on Kyushu Island, south-western Japan (Fig. 1). Planted conifers covered complex terrain, with Japanese cypress (*Chamaecyparis obtusa*) stands on a ridge area, and Japanese cedar (*Cryptomeria japonica*) extending from valley to hillside. We basically used 2 years of wind component data obtained in 2007 and 2008 to determine each fixed coordinate system. The analysis period for comparison and examination of flux data was August 8–September 17 2008; mean air temperature and total precipitation during the period were 28.6 °C and 420 mm, respectively.

Measurements were made on a 50-m tall meteorological tower. An albedo meter (CM 14, Kipp & Zonen, Delft, The Netherlands) and two pyrgometers (CG 3, Kipp & Zonen)

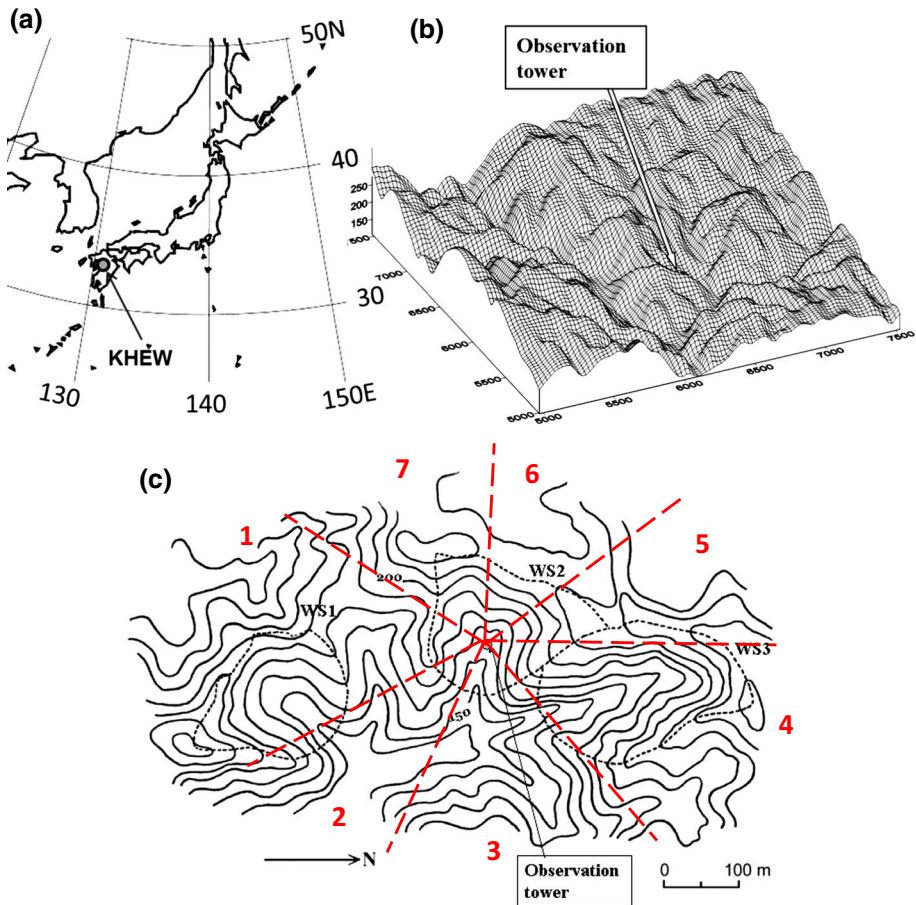


Fig. 1 Maps of the Kahoku experimental watershed (KHEW): **a** location; **b** surface map, derived from the “Takaigawa” digital map with a 1/25000 scale published by the Geospatial Information Authority of Japan. Vertical scale is exaggerated by a factor of three; **c** topographic map modified from Fig. 1 in Shimizu (2007). Dotted line and numbers show the seven sectors used for the sector-wise planar fit system

were placed at 47.2 m height, to obtain upward and downward solar and longwave radiative fluxes, respectively, and hence net radiation R_n . We distinguished daytime and nighttime by downward solar radiation greater than or equal to zero, respectively. Soil heat flux, G , was obtained at 0.05-m depth (including about 0.04 m of litter) near the tower, using a heat flux plate (HFT 3.1, REBS, Seattle, Washington, USA), with soil heat storage assumed negligible because of the low heat capacity of litter. Air temperature and relative humidity were obtained at two heights (42 and 20 m above the ground), using wet- and dry-bulb thermometers (ML-020L, EKO Instruments, Tokyo, Japan) and a temperature–humidity probe (HMP-45A, Vaisala, Helsinki, Finland), respectively. The thermo-hygrometers were ventilated with a fan in a stainless-steel shield. The dual-height measurements of temperature and water vapour were used to estimate the atmospheric heat storage (S_{air}).

A sonic anemo-thermometer (DAT-600 and TR-61C probe, Sonic Corporation; formerly Kaijo-Denki, Tokyo, Japan) and a gas intake mouth were installed at the top of the tower, with

a 0.15-m separation. Height above the ground (z) was 51.0 m. The sonic anemo-thermometer was extended on an aluminium alloy pole about 1.5 m from the tower, and its tilt was measured with a digital inclinometer (Pro360, Onset Computer Corp., Bourne, Massachusetts, USA). The tilt occurred only at 0.3° along the y -axis direction of the sonic anemo-thermometer. Sample air was drawn from the intake mouth into the closed-path infrared gas analyzer (IRGA: LI-7000, LI-COR, Lincoln, Nebraska, USA) through Teflon® tubes of 57-m length and 6-mm inner diameter from the mouth to the intake pump, and 3.5 m of a 4-mm tube between the pump and IRGA through a solenoid. Flow rate was monitored continuously (SEF-405, Horiba Stec, Kyoto, Japan) and was $7\text{--}8\text{ l min}^{-1}$ under normal conditions. Thus, the typical Reynolds numbers were in the range 1650–1900 in the broader tube and 2470–2830 in the narrower tube. The IRGA was calibrated about once per week by manually switching the flow paths of sample and reference gases. This configuration nearly matched that of Shimizu (2007), except for the distance between the intake mouth and the sonic anemo-thermometer, an upgraded IRGA, and removal of the dehumidifier and flow controller. Analogue signals from the sonic anemo-thermometer and IRGAs were recorded at 10 Hz, using a data logger (DR-M3b, TEAC, Tokyo, Japan).

A relatively large offset error was found in the raw analogue output signal of vertical axis wind velocity from the sonic anemo-thermometer during the analysis period. This error was almost constant (-0.066 m s^{-1}), based on a test in which the sonic anemo-thermometer probe was encased in a plastic bag. Although the main cause of this offset was not determined, we used $w_s = w_m + 0.066$, where subscript m is the measured raw output from the instrument, including the offset error. Note that the corrected w_s values (in m s^{-1}) were applied to determine all of the fixed coordinate systems and to calculate the fluxes used in this study, unless otherwise noted.

Average values and fluctuations in wind velocity components were calculated after a sonic transducer shadow correction for the TR-61C probe (Shimizu et al. 1999) and a sonic tilt correction based on the inclinometer measurement, applying 30-min block averages. All 30-min average values obtained in 2007 and 2008 were used to set the fixed coordinate systems, except the data screened out with the 5% threshold over-range values and data spikes. Scalar fluctuations were also calculated, using a 30-min block average.

The calculated fluxes were screened additionally using quality control based on Foken et al. (2004). A steady-state test for the measured flux was carried out as a quality control, and the difference in the integral turbulence characteristic value (i.e., normalized standard deviations using u_* or a scalar dynamic parameter, σ_{wr}/u_* or σ_T/T_* for example) measured and modelled was examined. The index of relative non-stationarity (RN) was calculated as the steady-state test for the flux data as follows (Foken et al. 2004),

$$RN_{wx} = \left| \frac{\left(\overline{w'_r x'} \right)_{wh} - \left(\overline{w'_r x'} \right)_{a6}}{\left(\overline{w'_r x'} \right)_{wh}} \right|, \quad (2)$$

where x is a particular wind component or scalar, the subscript wh is the covariance calculated using all averaged time-series data (here, 30 min), and the subscript $a6$ is the average of the covariance values calculated by dividing the time series six times equally (here, 5 min). The normalized standard deviations modelled obtained from previous studies were compiled by Foken (2008a), and are basically a power function of Obukhov length (L), with general form,

$$\frac{\sigma_x}{X_*} = c_1 \left| \frac{z-d}{L} \right|^{c_2}, \quad (3)$$

Table 1 Data classification based on the quality control guidelines of Foken et al. (2004)

QC class	Steady state test: <i>RN</i> in Eq. 2	Difference between measured and modelled normalized standard deviations	Horizontal wind angle to the sonic anemo-thermometer (SAT)
1	<0.3	<75 %	Other than from backyard (165–195°)
2	0.3–1.0	<100 % except class-1 data	
3	1.0–10	<1000 % except class-1 and -2 data	
4	>10 ^a	>1000 % ^a	165–195° ^a

^a The data were included in class-4 if one or more conditions apply

where σ is the standard deviation, and X_* is equal to u_* when x is u_r or w_r , and is a dynamic parameter when x is a scalar, as mentioned above. Zero-plane displacement (d) was determined to calculate the root-mean-square error (*RMSE*) from the modelled value at the minimum. Its value was 28.2 ± 0.2 m among all coordinate systems. Note that c_1 and c_2 are parameters dependent on $(z - d)/L$ and x (Foken et al. 2004; Foken 2008a). The same parameters were applied for scalars (T , χ_H , and χ_C , where χ is the mixing ratio to dry air, and the subscripts H and C are water vapour and CO₂, respectively), and the function diverged under near-neutral conditions. Thus, we did not examine the normalized standard deviations for the scalars when $(|z - d|/L)$ was < 0.005 . The following equations were applied for wind components (u_r and w_r) under slightly stable conditions ($0 < (z - d)/L \leq 0.4$) (Thomas and Foken 2002),

$$\sigma_w/u_* = 0.21 \ln \left(\frac{z+f}{u_*} \right) + 3.1, \tag{4a}$$

$$\sigma_u/u_* = 0.44 \ln \left(\frac{z+f}{u_*} \right) + 6.3, \tag{4b}$$

where $z_+ = 1$ m, and f is the Coriolis parameter. The quality control thresholds are shown in Table 1. The class-1 data were compared for further analysis, although the lower classes of data are shown occasionally as a reference. The total of the class-1 data generally occupied about 40 % of the daytime and < 10 % of the nighttime data.

High-frequency loss of closed-path CO₂ flux was corrected theoretically (Shimizu 2007). An additional correction is needed for the closed-path H₂O flux, particularly that obtained under high relative humidity (or low vapour pressure deficit D) conditions (Ibrom et al. 2007a, b). The parameters to correct the KHEW data in this study were determined preliminarily using the data obtained before the analysis period. Details are given in the Appendix.

3 Coordinate Rotation Systems and Their Comparison

The coordinate rotation systems applied for comparison herein are presented in Table 2, where all of these methods, except the double rotation, involve fixed coordinate systems. We outline two prevailing approaches, such as the double rotation and planar fit, as described in several other studies. Each fitting plane in the sector-wise planar fit is determined by the same procedure as the planar fit, and here we used seven planes with reference to average

Table 2 Coordinate rotation systems used in the comparison

Method	Procedure	Reference
Double rotation (DR)	Pitch angle is set for ($\overline{w_r} = 0$), for each averaging time	Kaimal and Finnigan (1994)
Planar fit (PF)	The coordinate plane is established through the linear regression applied to the time averaged three-dimensional sonic wind velocity components ($\overline{U_s}$, $\overline{v_s}$, $\overline{w_s}$) for a certain period	Wilczak et al. (2001)
Sector-wise planar fit (SPF)	Same as PF but multiple planes are applied for divided wind sectors	e.g. Paw et al. (2000); Yuan et al. (2007); Ono et al. (2008); Mildenerberger et al. (2009)
Lee's method (Lee's)	For every 10 wind direction sectors, $\overline{w_s} = a_{L1} + a_{L2}(\overline{u_s^2} + \overline{v_s^2})^{0.5}$ is determined, then the pitch angle θ determined as $\tan^{-1}[a_{L0}/(\overline{u_s^2} + \overline{v_s^2})^{0.5} + a_{L1}]$	Lee (1998)
Polynomial fit (Poly)	The θ is determined from the approximate 5th-order polynomial, which is set toward the plots of wind direction versus mean vertical angle at the sonic anemo-thermometer, $\tan^{-1}[\overline{w_s}/(\overline{u_s^2} + \overline{v_s^2})^{0.5} + a_{L1}]$	Shimizu (2007)
Moving average (MA)	The θ is determined from ensemble average of mean vertical angle at the sonic anemo-thermometer obtained under the condition of $(\overline{u_s^2} + \overline{v_s^2})^{0.5} \geq 0.5 \text{ m s}^{-1}$. The averaging range is $\pm 7.5^\circ$ of the horizontal wind direction	Su et al. (2004); Vickers and Mahrt (2006)
Ratio of wind components' moving average (RMA)	The $\tan \theta$ is determined from the ratio of ensemble average of $\overline{w_s}$ to that of $(\overline{u_s^2} + \overline{v_s^2})^{0.5}$ without wind speed threshold. The averaging range is same as MA	This study

vertical wind components on the single plane determined by the planar fit using two years of wind data (Fig. 2a). As a result, $\overline{w_r}$ in the sector-wise planar fit system decreased remarkably for all wind directions (Fig. 2b).

Besides the aforementioned three systems, the following four systems were tested, and in three of these the pitch rotation angle (θ) was determined from the mean vertical angle for the sonic anemo-thermometer obtained during the two-year period. The coefficients a_{L0} and a_{L1} in the following linear regression function in Lee (1998) were determined for every 10° wind sector,

$$\overline{w_s} = a_{L0} + a_{L1}\overline{U_s}, \quad (5)$$

where $\overline{U_s} = \sqrt{\overline{u_s^2} + \overline{v_s^2}}$. Then, θ was determined as

$$\tan \theta = \frac{(a_{L0} + a_{L1}\overline{U_s})}{\overline{U_s}} = \frac{a_{L0}}{\overline{U_s}} + a_{L1}. \quad (6)$$

As this system is the same as that of Lee (1998), it is henceforth referred to as "Lee's method". The constant offset error in w_s directly increases or decreases a_{L0} and affects θ .

Kosugi et al. (2007) and Shimizu (2007) considered θ as a dependent variable of wind direction ϕ , although they did not provide detailed procedures. They plotted $\overline{w_s}/\overline{U_s}$ with ϕ and conducted a regression analysis to determine the coefficients in the following,

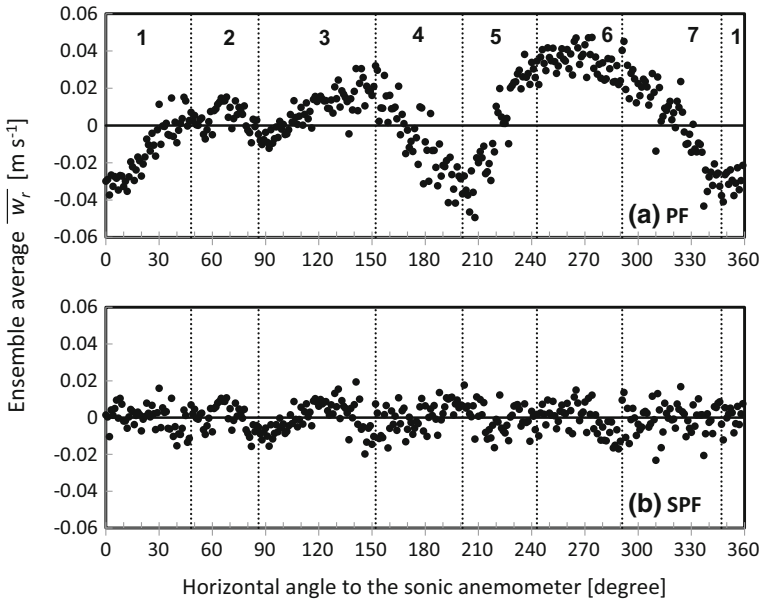


Fig. 2 Vertical wind-speed components ($\overline{w_r}$) for planar fit (a) and the sector-wise planar fit (b) set using the 2-year wind dataset (obtained 2007–2008) to the horizontal angle of the sonic anemo-thermometer. Values were ensemble averaged by 1° . Dotted lines and numbers correspond to the sectors in Fig. 1c

$$\frac{\overline{w_s}}{\overline{U_s}} = \sum_{k=0}^n a_{Kk} \varphi^k. \tag{7}$$

Kosugi et al. (2007) separated wind direction into five sectors from an overview of ϕ versus $\overline{w_s}/\overline{U_s}$ plots, and determined linear function coefficients ($n = 1$ in Eq. 7) for each section. Shimizu (2007) established a polynomial equation ($n = 5$ in Eq. 7) for all ϕ , so we adopted that equation for the test used herein, and call it the “polynomial fit”. Once the coefficients were obtained, θ was determined for all ϕ by calculating the arctangent of the right side of Eq. 7. The constant offset error affects all a_{Kk} .

Vickers and Mahrt (2006) developed a simpler approach to determine θ , as

$$\tan \theta = \langle \overline{w_s}/\overline{U_s} \rangle, \tag{8}$$

where the angled brackets denote the ensemble average of the corresponding wind sector. The offset error in w_s directly affects θ estimation by Eq. 8. Vickers and Marht removed the weak mean flow condition ($\overline{U_s} < 0.5 \text{ m s}^{-1}$) from the ensemble average calculation, and we followed their procedure. They separated wind direction into 36 sectors (every 10°). The approach of Su et al. (2004), which was a moving average of the wind sector for all ϕ , was considered more continuous. Therefore, we used Eq. 8 and a moving average of $\pm 7.5^\circ$, which is designated the “moving average”. Note that we used the 30-min block average $\overline{w_s}$ and $\overline{U_s}$ to regulate pitch angle of the method; we did not use the moving average of the 10-Hz data.

In the aforementioned three systems, the mean vertical angles at the sonic anemo-thermometer were referenced to determine θ . We provide another moving average procedure, in which θ is calculated from the ratio of the sonic anemo-thermometer mean vertical wind component to the horizontal wind component,

$$\tan \theta = \langle \overline{w_s} \rangle / \langle \overline{U_s} \rangle. \quad (9)$$

The ensemble average of the numerator and that of the denominator are calculated independently on the right-hand side of Eq. 9. In contrast to the moving average, all two years of wind data, except those including more than 5 % of the spikes plus over-range values, were used to establish the coordinate system, regardless of wind speed. This system is called the “ratio of components’ moving average”.

The examination proceeded according to the following process. First, fluxes on each coordinate system were compared, setting the traditional double rotation as the interim standard. Momentum fluxes $\overline{u'_i w'_i}$ were used to show how the basic turbulence quantities were altered by the coordinate rotation system. Total heat fluxes, sensible heat flux H plus latent heat flux λE , where λ is the latent heat of vapourization and E is the evapotranspiration, were compared from the standpoint of energy balance closure. The energy imbalance was minimal in summer (see Shimizu et al. 2015): the sum of the class-1 heat flux data ($H + \lambda E$) estimated by the double rotation over the 40-day analysis period at the KHEW site was 98 % of $(R_n - G - S_{\text{air}})$, with $R^2 = 0.69$. Note that the effect of atmospheric heat storage on the comparison was slight: the total was about 0.06 % of $H + \lambda E$. The CO_2 fluxes (F_c) were also compared, separating the data into those obtained during the daytime and nighttime.

Second, we applied σ_x / X_* values calculated in each system to examine agreement with Eqs. 3 and 4. Deviations from the equations were summarized using values of $RMSE$, calculated separately for the daytime and nighttime data. As Eqs. 3 and 4 were derived from relatively ideal conditions, the errors were used to determine the system that was physically more appropriate under each condition. In other words, when σ_x / X_* calculated in a given coordinate system better agreed with the estimate from Eqs. 3 or 4, it was assumed that the wind data transformed by the system were closer to those obtained under ideal conditions.

We also checked the effect of the sonic anemo-thermometer vertical wind velocity offset error on estimated fluxes, assuming a constant experimental offset value of -0.066 m s^{-1} , which corresponds to applying the real offset that occurred in the measurement. As a given constant offset error should have no impact on the flux estimate using the planar fit and the sector-wise planar fit, those procedures were excluded from the examination. Furthermore, we compared fluxes calculated for the six fixed systems other than the double rotation by using two years of wind data and the 40-day wind dataset to check the effect of dataset length on the flux estimate.

Based on these results, we discuss which system is appropriate for our observation site for both daytime and nighttime.

4 Results

4.1 Difference in Fluxes

We plotted the class-1 quality controlled data to compare fluxes calculated for each coordinate system and used the class-2 and class-3 data as a reference. The number of flux data regarded as class-1 data varied slightly with the coordinate system used (Fig. 3). The planar fit was most likely to pass the quality control filter, with the sector-wise planar fit second; the number of class-1 data was 2.4 % less than the planar fit. The moving average, the ratio of the components’ moving average, the polynomial fit, and Lee’s method were within several percentage points. Using the double rotation resulted in the smallest number of class-1 data, which was 9.5 % smaller than when using the planar fit system.

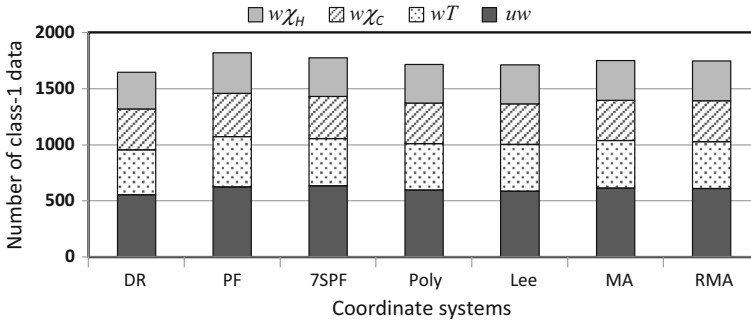


Fig. 3 Numbers of flux data passing the class-1 quality control criteria in Table 2 for each coordinate system. The abbreviations uw , wT , $w\chi_H$, and $w\chi_C$ correspond to momentum fluxes caused by main flow (u), sensible and latent heat fluxes, and CO_2 fluxes, respectively. Abbreviations under the vertical axis correspond to each coordinate system in Table 1. *DR* double rotation coordinate system, *PF* planar fit, *SPF* sector-wise planar fit, *Lee*'s Lee's method, *Poly* polynomial fit, *MA* moving average, *RMA* ratio of the components' moving average

The comparison of the momentum fluxes $\overline{u'_r w'_r}$ are shown in Fig. 4 as an example, using those with the double rotation as x -axis values. Orthogonal regression was carried out for the comparison. The regression line and the equation correspond to the relationship between the class-1 data calculated by the double rotation and those by the compared system, which is common for the following comparisons. The $\overline{u'_r w'_r}$ values were linearly correlated with each other, with regression slopes of 0.93–0.99, except the smaller slope using the sector-wise planar fit, suggesting an underestimate of $\overline{u'_r w'_r}$.

The trends in total heat flux $H + \lambda E$ and F_c during the daytime were similar to the $\overline{u'_r w'_r}$ comparison, although the determination coefficient was slightly larger, and the slope of the regression approached unity for each comparison (Table 3). However, the table shows that the absolute values of $H + \lambda E$ and F_c in the daytime calculated by the double rotation were slightly larger by about 5% than those calculated by the sector-wise planar fit. This result suggests that the energy imbalance at the KHEW site would expand slightly with use of the sector-wise planar fit, even though the coordinate planes were set using the two-year wind dataset, and the data were selected by strict quality control.

The plots were greatly scattered for F_c obtained during the nighttime, when comparing the double rotation with the planar fit and the sector-wise planar fit, although the number of data compared was rather small (Fig. 5). The sector-wise planar fit underestimated F_c by about 7% relative to that of the double rotation, indicating that the difference between the sector-wise planar fit and the other systems may have been greater during the nighttime. It was more noticeable in the F_c values than in the heat and momentum fluxes because the absolute value of nighttime ecosystem respiration is usually within a comparable range to daytime net ecosystem exchange, in contrast to the heat and momentum fluxes.

4.2 Normalized Standard Deviations of the Wind Components and Scalars

The measured σ_w/u_* and σ_T/T_* values calculated by the double rotation, the sector-wise planar fit, and the ratio of the components' moving average are plotted against the modelled values in Fig. 6 as examples. The data were the class-1 quality controlled data. Small differences were found between the coordinate rotations, although the nighttime values seemed relatively scattered using the double rotation. A comparison of the *RMSE* values from the values modelled by Eqs. 3 and 4 supported the general impression of the figures, particularly

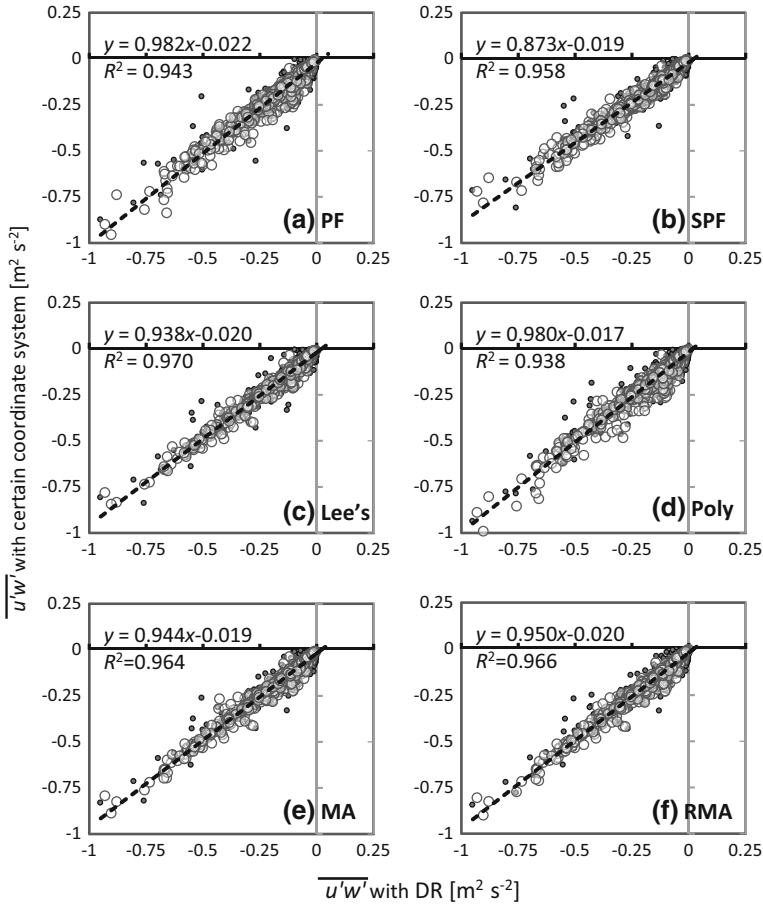


Fig. 4 Comparison of $\overline{u'_r w'_r}$ momentum flux calculated by each coordinate rotation system with those calculated by the double rotation coordinate system (DR). Fluxes calculated by: **a** the planar fit (PF), **b** the sector-wise planar fit (SPF), **c** Lee's method (Lee's), **d** the polynomial fit (Poly), **e** the moving average (MA), and **f** the ratio of the components' moving average (RMA) in Table 1. *White and black circles* are data that passed the class-1 quality control criterion and the class-2 and -3 data in Table 2, respectively. *Dotted lines* are the orthogonal regression carried out using the class-1 data

that obtained during daytime (Table 4). The best σ_x / X_* values did not differ by 5% from the second best values in the daytime. Meanwhile, the $RMSE$ values for the nighttime σ_T / T_* using the sector-wise planar fit became smaller by about 9% than that in all of the other systems. The $RMSE$ in $\sigma_{\chi C} / C_*$ also became the smallest using the sector wise-planar fit, although the difference from the planar fit was slight. These results suggest that the redistribution of wind components using the sector-wise planar fit at night caused the KHEW scalar flux data to be nearer to the flat and homogeneous surface condition for which the aforementioned theories were obtained. The sector-wise planar fit for σ_u / u_* during daytime also agreed better with the equation but use of the sector-wise planar fit for the daytime scalar fluxes resulted in worse agreement, although the differences from the other systems were slight.

Table 3 Correlation parameters for the comparisons between momentum flux ($\overline{u'_t w'_t}$), sum of heat fluxes ($H + \lambda E$), and CO₂ flux obtained during daytime, calculated in each system with those calculated by double rotation

	$\overline{u'_t w'_t}$ ($\text{m}^2 \text{s}^{-2}$)		$H + \lambda E$ (W m^{-2})		F_c (daytime) ($\text{mgCO}_2 \text{ m}^{-2} \text{ s}^{-1}$)		F_c (nighttime) ($\text{mgCO}_2 \text{ m}^{-2} \text{ s}^{-1}$)					
	R^2	Slope	Interception	R^2	Slope	Interception	R^2	Slope	Interception			
PF	0.943	0.982	-0.022	0.971	0.977	11.675	0.961	0.987	-0.175	0.742	0.836	1.356
SPF	0.958	0.873	-0.019	0.970	0.933	12.756	0.960	0.943	-0.141	0.902	0.744	1.190
Lee's	0.970	0.938	-0.020	0.982	0.980	3.568	0.980	0.988	-0.070	0.963	0.901	0.762
Poly	0.938	0.980	-0.017	0.973	0.985	5.240	0.968	0.979	-0.118	0.910	0.877	0.925
MA	0.964	0.944	-0.019	0.980	0.990	4.341	0.977	0.983	-0.050	0.953	0.892	0.812
RMA	0.966	0.950	-0.020	0.978	0.990	5.013	0.977	0.985	-0.067	0.949	0.888	0.851

An orthogonal regression was conducted for data passing the class-1 quality control filters shown in Table 2

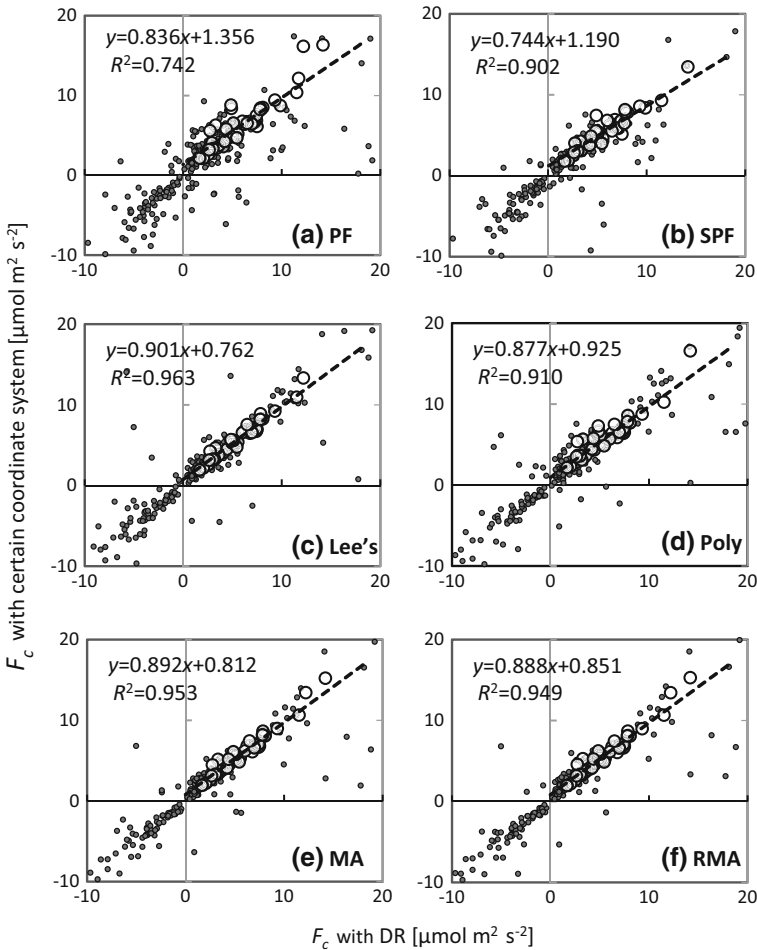


Fig. 5 Comparison of nighttime CO_2 fluxes (F_c) obtained using each system. Markers and dotted lines in panels (a–f) are the same as in Fig. 4

4.3 Impact of Offset Error on Sonic Vertical Wind Velocity

When the planar fit or the sector-wise planar fit was used for the flux calculations, the constant offset error in w_s did not cause differences in the calculated fluxes based on their original definitions. Consequently, the impact of offset error was checked for the other five systems, except the planar fit and the sector-wise planar fit.

Figure 7 compares F_c calculated after eliminating a -0.066 m s^{-1} offset error in w_s from the sonic vertical velocity values with those calculated from raw values, on the assumption $w_s = w_m$ in each coordinate rotation system. The results indicate that the aforementioned offset error often caused large errors in F_c for all systems. In particular, the average error was around 30% for the polynomial fit, even using only the class-1 data for comparison. The errors were 5–10% for the other systems, and the error rate exceeded or equalled the underestimate of the sector-wise planar fit. The same tendency occurred in $H + \lambda E$, although

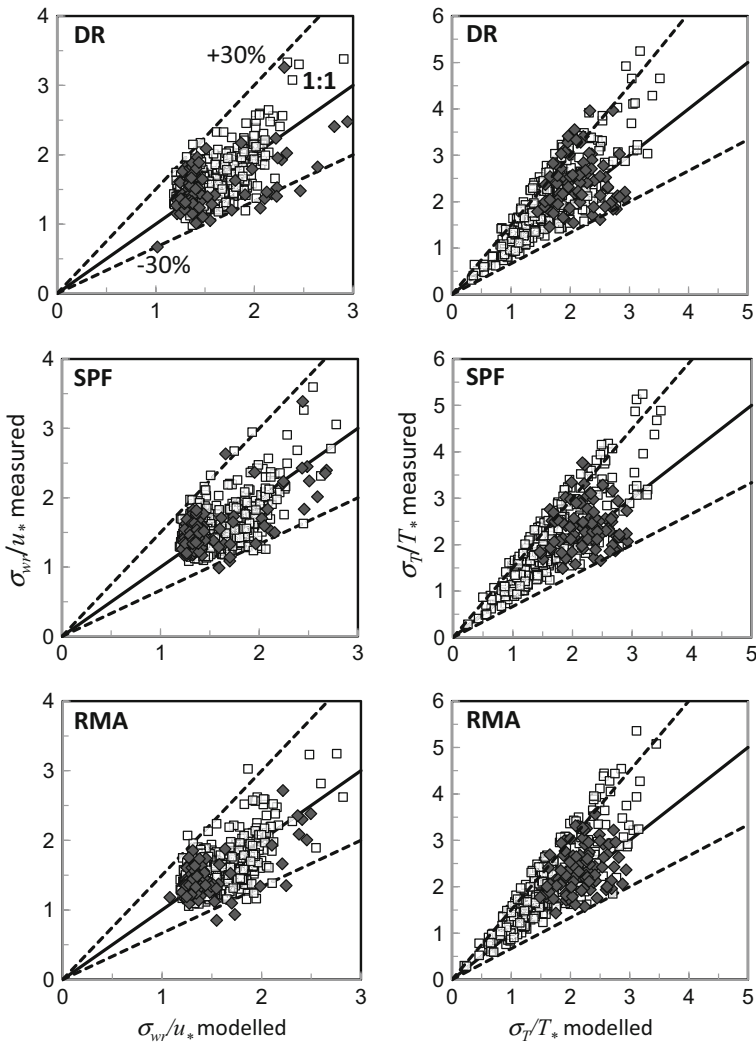


Fig. 6 Examples of σ_w/u_* (left panels) and σ_T/T_* (right panels) plots modelled by Eqs. 3 and 4 in the text (horizontal axis) and measured in the three coordinate systems: the double rotation (DR, upper panels), the sector-wise planar fit (SPF, middle panels), and the ratio of the components' moving average (RMA, lower panels). The class-1 quality controlled data are plotted. Solid and dotted lines are the 1:1 line and the $\pm 30\%$ lines, respectively. White and black squares correspond to daytime and nighttime, respectively

the figures are not shown. However, the errors in F_c were larger, and the plots were scattered more than those in $H + \lambda E$, suggesting that the impact of offset error in w_s on F_c was stronger than that on the heat fluxes.

4.4 Effect of Dataset Length on Fluxes for Framing Each System

The differences in fluxes caused by dataset length to set the fixed-method parameters were also examined. The F_c errors were generally not large for any of the coordinate systems when

Table 4 Root-mean-square errors of the measured normalized standard deviations for friction velocity or the scalar dynamic parameters in each system from the values estimated using Eqs. 3 or 4 in the text

	Daytime					Nighttime				
	σ_w/u_*	σ_u/u_*	σ_T/T_*	$\sigma_{\chi C}/\chi C_*$	$\sigma_{\chi H}/\chi H_*$	σ_w/u_*	σ_u/u_*	σ_T/T_*	$\sigma_{\chi C}/\chi C_*$	$\sigma_{\chi H}/\chi H_*$
DR	0.273	1.295	0.544†	0.688†	0.659	0.317**	0.586†	0.684**	0.860	N/A
PF	0.258†	1.344**	0.578	0.750	0.666	0.268	0.761	0.587	0.804	N/A
SPF	0.279	1.279†	0.568	0.754**	0.680**	0.258	0.786	0.535†	0.800†	N/A
Poly	0.279	1.322	0.597**	0.737	0.638†	0.276	0.791**	0.651	0.856	N/A
Lee	0.279	1.318	0.596	0.709	0.656	0.197†	0.598	0.605	0.857	N/A
MA	0.308**	1.289	0.589	0.721	0.647	0.210	0.701	0.632	0.879**	N/A
RMA	0.262	1.298	0.582	0.729	0.655	0.224	0.617	0.580	0.871	N/A

† and ** indicate the best and the worst in the category, respectively
 N/A < 5 % of data were available

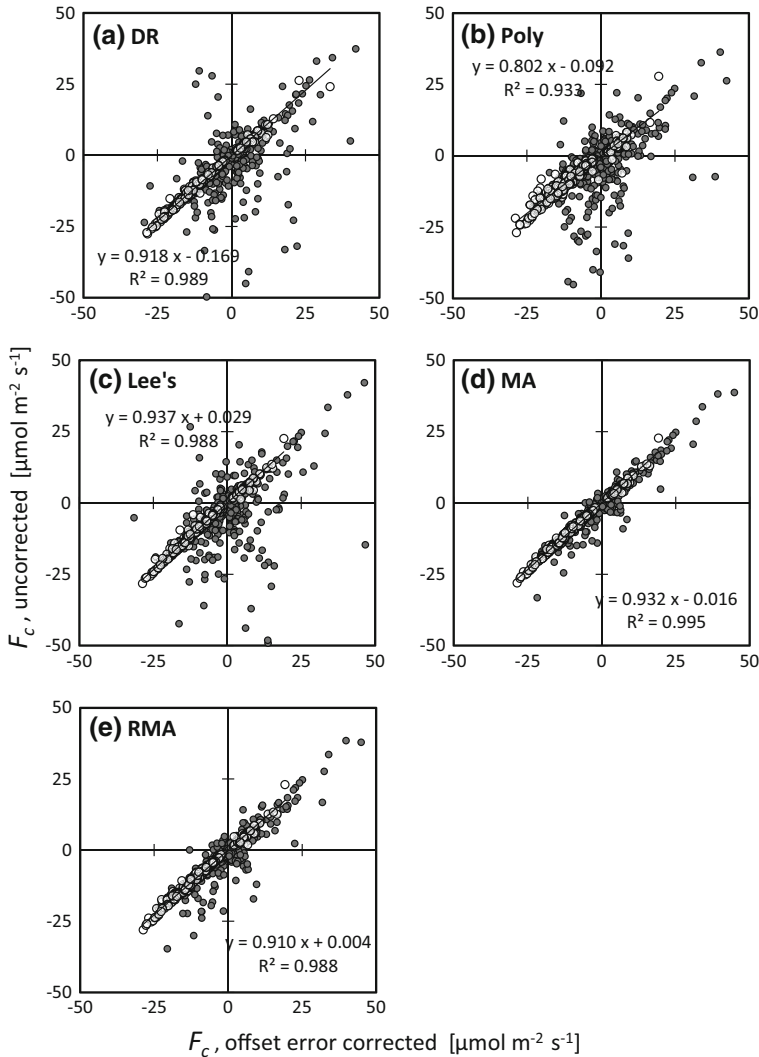


Fig. 7 Effect of the sonic vertical wind component offset error on flux values calculated with each coordinate system: **a** double rotation (DR); **b** Lee's method (Lee's); **c** polynomial fit (Poly); **d** moving average (MA); and **e** the ratio of the components' moving average (RMA). Assumed offset error is 0.066 m s^{-1} . *Left and right panels are comparisons of $H + \lambda E$ and F_c , respectively. White and black circles are the same as in Fig. 4*

the fluxes were calculated in a certain system set by using the 40-day wind data and when they were calculated in the system set by two-year wind data (Fig. 8). These F_c errors were within 2% for all systems when comparing the class-1 data. In particular, the average error remained within 2% for the planar fit and the ratio of the components' moving average after including the class-2 and class-3 data. This held true for $H + \lambda E$ in all coordinate systems: the difference in the length of the dataset period, 40 days and two years for each system, only slightly affected the calculated heat flux values. The F_c error in the planar fit was much smaller than expected from a previous study (Siebicke et al. 2012), and it could be attributed

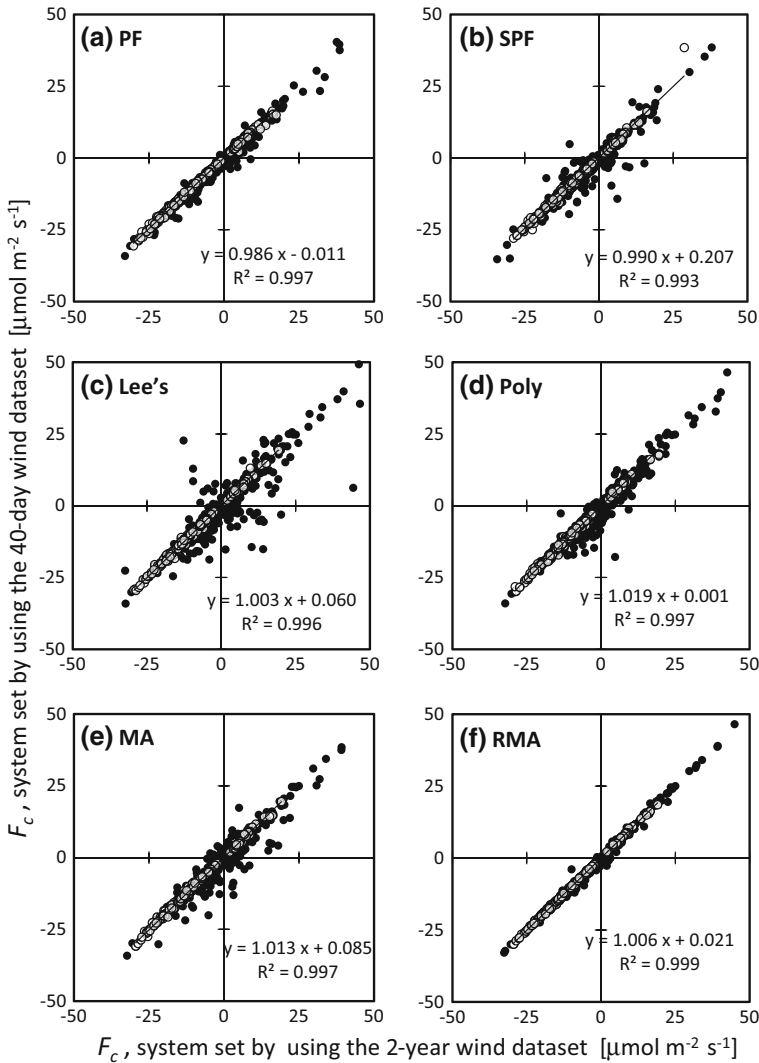


Fig. 8 Effect of dataset length for determining the effect of each fixed system on F_c values. Daytime and nighttime data are mixed in the same figure. Systems fixed by the two-year wind data (horizontal axis) and by the 40-day wind data are compared. **a** The planar fit (PF); **b** the sector-wise planar fit (SPF); **c** Lee's method (Lee's); **d** the polynomial fit (Poly); **e** the moving average (MA); and **f** the ratio of the components' moving average (RMA). Markers are the same as in Fig. 4

to a difference in observation site characteristics. The one to two months of wind data were sufficient at our site (KHEW) to set parameters for every fixed system considered here.

5 Discussion

Given that our comparisons were carried out at only one site, it is difficult to determine the best coordinate system for any complex terrain. However, the optimum coordinate system for our site can be addressed from practical and conceptual points of view.

5.1 The Planar Fit and the Sector-Wise Planar Fit

The planar fit was no worse than the other systems considered in this study for our site and the 40-day analysis period: the number of class-1 quality controlled data became the maximum when using the planar fit, and the energy imbalance and the errors from modelled σ_x/X_* were not extended by using the planar fit. However, the planar fit applies only one fitting planar, as it was originally developed as an instrumental tilt correction method by Wilczak et al. (2001). Thus, it is inadequate to analyze airflow across complex terrain (e.g. Vickers and Mahrt 2006). Additionally, the system may be inadequate for instrumental correction as reported by Ono et al. (2008) and Li et al. (2013). In our case, backward flow from the sonic anemo-thermometer was distorted (Wieser et al. 2001), even after correcting the transducer shadow. Furthermore, Rebmann et al. (2012) indicated that the time and stability class should be well selected for setting the single planar. This may not be a limitation of the planar fit, but may make it difficult to apply this system for long-term measurements.

In contrast, using the sector-wise planar fit can solve these issues. This system covers complex terrain with multiple coordinate planes, and the average w_r approaches zero for nearly all wind directions. Siebicke et al. (2012) successfully estimated nighttime net ecosystem exchange including advection terms using the sector-wise planar fit. Li et al. (2013) reported that the system is suitable to mitigate the effect of instrumental flow distortion on flux calculations. These results support the conclusion that the sector-wise planar fit is the best system for certain types of complex terrain.

Nevertheless, fluxes calculated with the sector-wise planar fit were underestimated relative to those from all other systems. A similar result was obtained in a comparison between the double rotation, the planar fit, and the sector-wise planar fit for complex terrain at the Gwangneung Forest site in South Korea (Yuan et al. 2007, 2011). This underestimation remained in our data, even after applying the two-year wind data to set the division of sectors and their parameters as in Siebicke et al. (2012) and after applying a strict quality control method (Foken et al. 2004). The systematic underestimate linearly reduced 5–7% of the fluxes with large absolute values during daytime, i.e., momentum and heat fluxes and daytime F_c . The energy imbalance was exacerbated by about 5% using the system.

The causes for the flux underestimate that occurred using the sector-wise planar fit were examined. As a result of the σ_{wr} comparison in Fig. 9, the values were underestimated when using the sector-wise planar fit. However, the difference in σ_{wr} of the sector-wise planar fit from that of the other systems was smaller than the difference in momentum and scalar fluxes. Figure 10 shows the ensemble average for the lag correlation between u'_t and w'_t calculated with the sector-wise planar fit, the double rotation, and the ratio of the components' moving average. The figure shows that the correlation between u'_t and w'_t was slightly smaller in the sector-wise planar fit with a short lag time, whereas no systematic cause for the larger calculated flux was found in the double rotation or the ratio of the components' moving average at longer lag times. These results suggest that the accumulation of smaller w' and the smaller correlation between w' and x' in the sector-wise planar fit than those of the other systems was the main cause for the difference in daytime fluxes, whereas overestimates by other systems relative to the sector-wise planar fit were not likely a cause. Furthermore, comparisons between daytime σ_x/X_* and Eqs. 3 and 4 did not show the superiority of the sector-wise planar fit. Although field measurements may not completely remove energy imbalance (e.g. Inagaki et al. 2006; Foken et al. 2006; Foken 2008b), a coordinate system that extends the problem would probably not be used without other clear advantages (e.g. Leuning et al. 2012). Therefore, the sector-wise planar fit is not the best coordinate system for daytime heat-flux calculations at the KHEW site, at least at present.

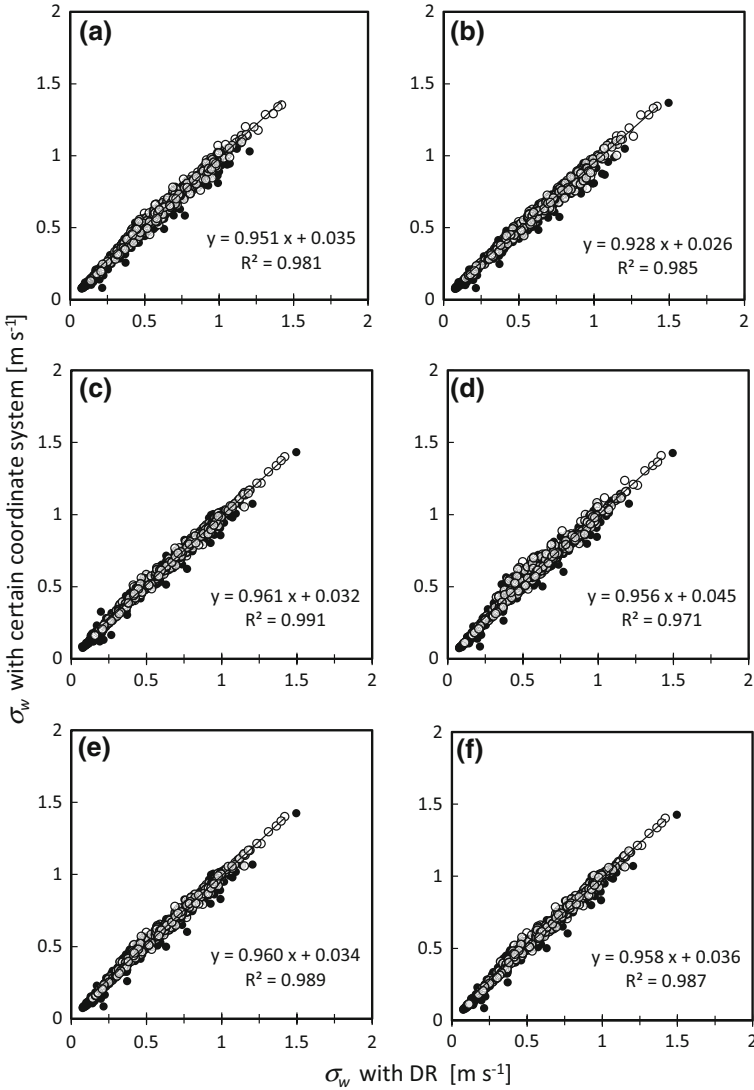


Fig. 9 Comparison of vertical velocity component standard deviation σ_{wT} for each system at the Kahoku experimental watershed over the entire study period. Panels (a–f), markers, and dotted lines are the same as in Fig. 4

The underestimate in nighttime F_c with the sector-wise planar fit was about 7%, which was similar to that of the daytime fluxes. However, the nighttime σ_T/T_* and $\sigma_{\chi C}/C_*$ values using the sector-wise planar fit were closer to Eq. 3 than to the other systems. These results coincide with Siebicke et al. (2012), in which the sector-wise planar fit was recommended because nighttime F_c was estimated well using the system. Furthermore, nighttime $\langle \overline{w_T} \rangle$ was smaller and consistently near-zero for all wind directions when separately comparing $\langle \overline{w_T} \rangle$ using the sector-wise planar fit for daytime and nighttime (Fig. 11), whereas the values were occasionally large during daytime. This result suggests that nighttime fluxes are strongly affected by general topographic features because of a relatively large footprint and

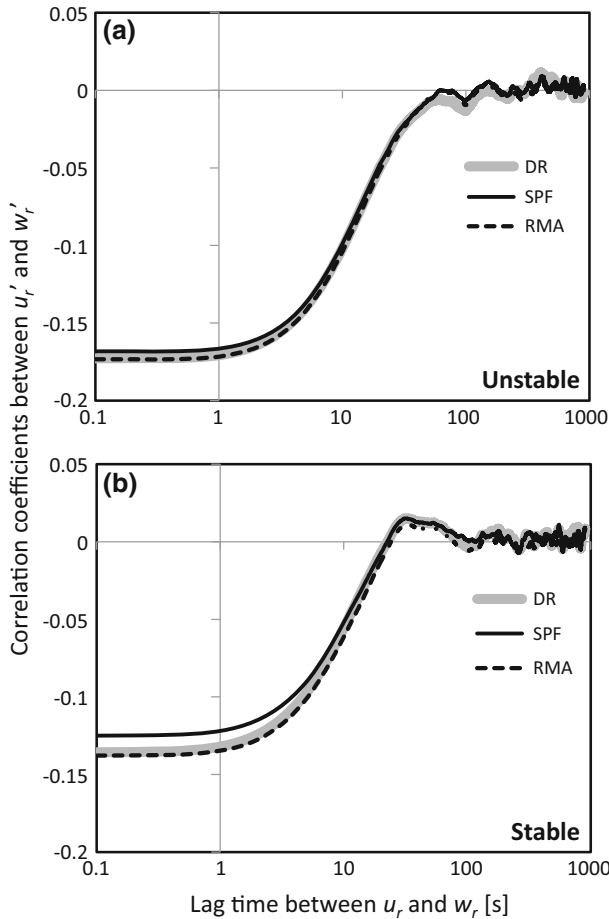


Fig. 10 Examples of the lag correlation between u'_r and w'_r for the three coordinate rotation systems: the double rotation (*thick gray lines*), the sector-wise planar fit (*black lines*), and the ratio of the components' moving average (*dashed lines*). Ensemble averaged class-1 quality controlled data are plotted and were obtained under **a** unstable and **b** stable conditions

suppressed vertical exchange. However, terrain details may influence daytime fluxes under unstable conditions with a smaller footprint. Thus, considering these favourable findings, the sector-wise planar fit was possibly the most effective system among all coordinate systems considered here for estimating nighttime fluxes at the KHEW site. The tower at this site was built near a valley, and the $z - d$ value was relatively small compared with the height of trees around the tower (larger near the valley) and the heights of surrounding ridges. Therefore, if the height or the location of the tower was changed, the sector-wise planar fit might have been the best choice for daytime data, even at our site.

5.2 Other Coordinate Systems

Because the sector-wise planar fit is not the first choice for daytime flux estimates and because planar fit is too simple to apply to complex terrain, we considered which of the other five coordinate systems would be suitable for estimating daytime fluxes at our site. Among them,

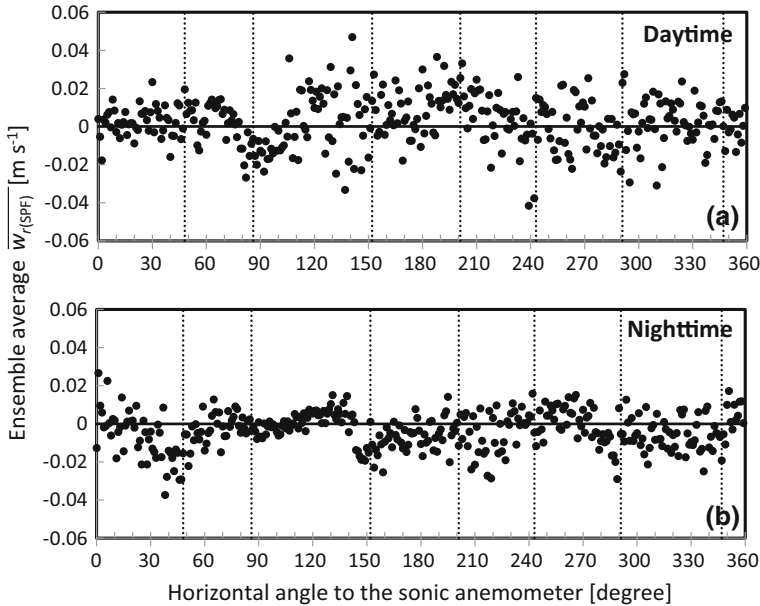


Fig. 11 Same as in Fig. 2b, but classifying the data obtained **a** during daytime and **b** nighttime. Ensemble average of $w_{r(SPF)}$ is recalculated for each period

the double rotation system was slightly worse than the other systems, based on the number of data passing the quality control process. However, either the double rotation or one of the four fixed systems without roll rotation was applicable overall, if class-1 data are applied for further analysis, and the w_s offset error can be removed before the flux calculation. If that error is assumed constant, we can detect it in the field test as described and/or by determining b_0 in the (sector-wise) planar fit for each period and comparing it with values from other periods. However, the offset error may sometimes occur without notice, because of an electric noise, blowing dust, and/or the inexact box calibration (ISO 2002). Calculated fluxes should be stable against the change in offset error with an optimal coordinate system. The fluxes calculated using the polynomial fit varied more than those calculated by other systems; therefore, the polynomial fit is slightly worse than the others. If a constant offset error cannot be obtained, such as when reanalyzing data acquired previously, the sector-wise planar fit should be the remaining choice even during the daytime because the offset error easily comprised 5–10% of the average flux calculation error.

Dataset length was not a major issue to determine the coordinate system for our site, if it was longer than 1–2 months. As our site is covered with evergreen trees and snowfall is rare, the leaf area index and colour of the leaf/ground surface does not substantially change throughout the year, and a wind dataset of one year or longer would be suitable to set a stable fixed system. However, if the site has many deciduous trees and/or is covered with snow during the winter, surface conditions can change dramatically within a month, and dataset length should be adjusted to that condition. Even in such cases, the double rotation was basically applicable, given that it is not necessarily erratic relative to the other systems, as in this study. The ratio of the components' moving average may also be applicable based on Fig. 8 because not only the class-1 data but also the class-2 and class-3 data were stable regardless of the length of the dataset period, although it may depend on site characteristics.

Among the six fixed systems, only the moving average applies the wind speed threshold as a data filter when setting the coordinate system. That is, data obtained for $\overline{U}_s < 0.5 \text{ m s}^{-1}$ were neglected when setting the system, although they might be regarded as acceptable if they pass the quality control process. If this is considered somewhat contradictory and/or a threshold value of 0.5 m s^{-1} as somewhat speculative, the ratio of the components' moving average should be substituted for the moving average.

6 Concluding Remarks

We examined the effect of coordinate systems on turbulence fluxes calculated over a forest in complex terrain. Seven systems were tested, including the newly proposed the ratio of the components' moving average. The calculated momentum fluxes, sensible plus latent heat fluxes, and CO_2 flux (F_c) during daytime were not significantly altered by the choice of coordinate system. The exception was the sector-wise planar fit, which always underestimated these fluxes by about 5%. The validity of the sector-wise planar fit was not confirmed based on the comparison of daytime normalized standard deviations with the previously obtained Eqs. 3 and 4. These results suggest that the sector-wise planar fit is not the optimum choice for estimating daytime fluxes, at least at our site (KHEW). The double rotation or one of the fixed systems without roll rotation were suitable systems for daytime flux calculations in complex terrain, if the constant offset error in the sonic anemo-thermometer vertical wind velocity is effectively avoided.

The sector-wise planar fit also underestimated nighttime F_c , but the tendency was different from the other fluxes. The comparison with F_c calculated using the double rotation was less correlated, with an average underestimate of about 7%. Nighttime σ_T/T_* and $\sigma_{\chi C}/C_*$ values obtained using the sector-wise planar fit were closer to the values modelled by Eq. 3 than those with the other systems. Furthermore, the nighttime \overline{w}_T ensemble averages using the sector-wise planar fit were more stable than those during daytime with the same system. These results suggest the potential of the sector-wise planar fit as a suitable system for estimating nighttime fluxes at the KHEW site, as suggested in a recent study (e.g. Siebicke et al. 2012).

Acknowledgments The author is deeply grateful to Dr. Akira Shimizu of the Kyushu Research Centre of the Forestry and Forest Products Research Institute (FFPRI-KYS) and to Dr. Koji Tamai of FFPRI and Dr. Tomo'omi Kumagai of Nagoya University for their cooperation with the field observations at the KHEW site. In addition, the author appreciates Prof. Masakazu Suzuki of The University of Tokyo for encouragement during this study. KHEW maintenance and management is supported by the Kyushu Regional Forest Office and FFPRI-KYS.

Appendix

High Frequency Correction for the Closed-Path H_2O Flux

Ibrom et al. (2007a) proposed that the closed-path H_2O fluctuation has an attenuated signal in the high frequency region, which is unaccountable based on previous correction theories (e.g. Shimizu 2007). Furthermore, Ibrom et al. (2007b) showed that a signal delay occurs in the closed-path H_2O data compared with that in the CO_2 data, although both were simultaneously taken from the sample mouth. We found a similar relationship between relative humidity or vapour pressure deficit (VPD) and the additional signal delay time in H_2O to that in CO_2 as Ibrom et al. (2007b) using the class-1 quality control data obtained in June–August 2007

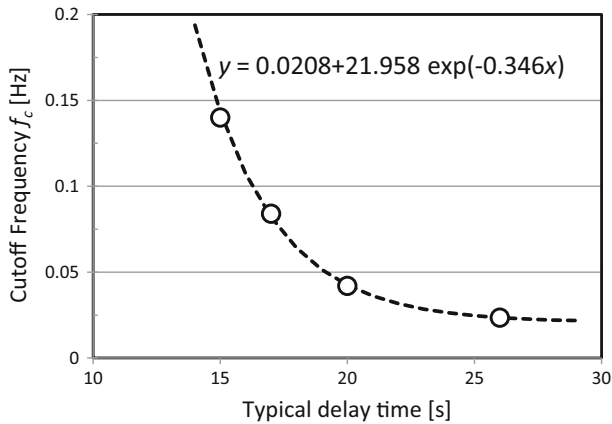


Fig. 12 Cut-off frequency (f_c) calculated from the normalized cospectral ratio of closed-path water vapour flux to sensible heat flux. *White circles* are bin-averaged of f_c by four ranges of delay time estimated from the maximum correlation that occurred. The *line* represents Eq. 10 in the text

and January–February 2008. The additional delay time was estimated to be 9.5 s when $VPD = 2.5$ hPa (figure not shown). First, the class-1 data were used to calculate the $w_r - \chi_H$ cospectrum after correcting for sensor separation, the line averaging effect (both in Moore 1986), and the volume averaging effect of the closed-path IRGA (Massman 2004). Then, the cut-off frequencies (f_c [Hz]) at which the magnitude of the normalized $w_r - \chi_H$ cospectrum became $(1/2)^{0.5}$ to that of the normalized $w_r - T$ cospectrum obtained simultaneously were compiled for four time ranges (14–16, 16–18, 18–22, and 22–30 s). The average f_c plotted against typical delay time is shown in Fig. 12; we obtained the relationship between delay time and f_c as,

$$f_c = 0.0208 + 21.958 \exp(-0.346 dt_H), \quad (10)$$

where dt_H is the delay time determined from the maximum correlation between w_r and closed-path χ_H . The f_c estimated from this equation was applied to the H₂O tube flow correction, instead of the theoretical equation.

References

- Aubinet M, Grelle A, Ibrom A, Rannik U, Moncrieff J, Foken T, Kowalski AS, Martin PH, Berbigier P, Bernhofer Ch, Clement R, Elbers J, Granier A, Grunwald T, Morgenstern K, Pilegaard K, Rebmann C, Snijders W, Valentini R, Vesala T (2000) Estimates of the annual net carbon and water exchange of forest: the EUROFLUX methodology. *Adv Ecol Res* 30:113–175
- Finnigan JJ (2004) A re-evaluation of long-term flux measurement techniques. Part II: coordinate systems. *Boundary-Layer Meteorol* 113:1–41
- Finnigan JJ, Clement R, Malhi Y, Leuning R, Cleugh HA (2003) A re-evaluation of long-term flux measurement techniques. Part I: averaging and coordinate rotation. *Boundary-Layer Meteorol* 107:1–48
- Foken T (2008a) *Micrometeorology*. Springer, Berlin 308 pp
- Foken T (2008b) The energy balance closure problem: an overview. *Ecol Appl* 18:1351–1367
- Foken T, Göckede M, Mauder M, Mahrt L, Amiro BD, Munger JW (2004) Post-field data quality control. In: Lee X, Massman WJ, Law B (eds) *Handbook of micrometeorology: a guide for surface flux measurement and analysis*. Kluwer, Dordrecht, pp 181–208
- Foken T, Wimmer M, Mauder M, Thomas C, Liebethal C (2006) Some aspects of the energy balance closure problem. *Atmos Chem Phys* 6:4395–4402

- Göckede M, Foken T, Aubinet M, Aurela M, Banza J, Bernhofer C, Bonnefond JM, Brunet Y, Carrara A, Clement R, Dellwik E, Elbers J, Eugster W, Fuhrer J, Granier A, Grünwald T, Heinesch B, Janssens IA, Knohl A, Koebler R, Laurila T, Longdoz B, Manca B, Marek M, Markkanen T, Mateus J, Matteucci G, Mauder M, Migliavacca M, Minerbi S, Moncrieff J, Montagnani L, Moors E, Ourcival J-M, Papale D, Pereira J, Pilegaard K, Pita G, Rambal S, Rebmann C, Rodrigues A, Rotenberg E, Sanz MJ, Sedlak P, Seufert G, Siebicke L, Soussana JF, Valentini R, Vesala T, Verbeek H, Yakir D (2008) Quality control of CarboEurope flux data—part 1: coupling footprint analyses with flux data quality assessment to evaluate sites in forest ecosystems. *Biogeosciences* 5:433–450
- Ibrom A, Dellwik E, Flyvbjerg H, Jensen NO, Pilegaard K (2007a) Strong low-pass filtering effects on water vapour flux measurements with closed-path eddy correlation systems. *Agric For Meteorol* 147:140–156
- Ibrom A, Dellwik E, Larsen SE, Pilegaard K (2007b) On the use of the Webb–Pearman–Leuning theory for closed-path eddy correlation measurements. *Tellus B* 59:937–946
- Inagaki A, Letzel O, Raasch S, Kanda M (2006) Impact of surface heterogeneity on energy imbalance: a study using LES. *J Meteorol Soc Jpn* 84:187–198
- ISO (2002) ISO 16622: Meteorology—Sonic anemometer/thermometer—acceptance test method for mean wind measurements, 21 pp
- Kaimal JC (1988) In: Mitsuta Y, Yamada M (trans) The atmospheric boundary layer—its structure. Lecture notes. Indian Inst TropicMet Visiting Professorship Program (in Japanese). Gihoudo Shuppan, Tokyo
- Kaimal JC, Finnigan JJ (1994) Atmospheric boundary layer flows. Oxford University Press, 289 pp
- Kosugi Y, Takanashi S, Tanaka H, Ohkubo S, Tani M, Yano M, Katayama T (2007) Evapotranspiration over a Japanese cypress forest. I. Eddy covariance fluxes and surface conductance characteristics for 3 years. *J Hydrol* 337:269–283
- Lee X (1998) On micrometeorological observation of surface–air exchange over tall vegetation. *Agric For Meteorol* 91:29–49
- Lee X, Finnigan JJ, Paw UKT (2004) Coordinate systems and flux bias error. In: Lee X, Massman W, Law B (eds) *Handbook of micrometeorology*. Kluwer, Dordrecht, pp 33–66
- Leuning R, van Gorsel E, Massman WJ, Isaac PR (2012) Reflections on the surface energy imbalance problem. *Agric For Meteorol* 156:65–74
- Li M, Babel W, Tanaka K, Foken T (2013) Note on the application of planar-fit rotation for non-omnidirectional sonic anemometers. *Atmos Meas Tech* 6:221–229
- Massman WJ (2004) Concerning the measurement of atmospheric trace gas fluxes with open- and closed-path eddy covariance systems: the WPL terms and spectral attenuation. In: Lee X, Massman WJ, Law B (eds) *Handbook of micrometeorology*. Kluwer, Dordrecht, pp 133–160
- McMillen RT (1988) An eddy correlation technique with extended applicability to non-simple terrain. *Boundary-Layer Meteorol* 43:231–245
- Mildenberger K, Beiderwieden E, Hsia YJ, Klemm O (2009) CO₂ and water vapor fluxes above a subtropical mountain cloud forest—the effect of light conditions and fog. *Agric For Meteorol* 149:1730–1736
- Moore CJ (1986) Frequency response corrections for eddy correlation systems. *Boundary-Layer Meteorol* 37:17–35
- Nakai T, van der Molen MK, Gash JHC, Kodama Y (2006) Correction of sonic anemometer angle of attack errors. *Agric For Meteorol* 136:19–30
- Ono K, Mano M, Miyata A, Inoue Y (2008) Applicability of the planar fit technique in estimating surface fluxes over flat terrain using eddy covariance. *J Agric Meteorol* 64:121–130
- Paw U KT, Baldocchi D, Meyers TP, Wilson KB (2000) Correction of eddy covariance measurements incorporating both advective effects and density fluxes. *Boundary-Layer Meteorol* 97:487–511
- Rebmann C, Kolle O, Heinesch B, Queck R, Ibrom A, Aubinet M (2012) Data acquisition and flux calculations. In: Aubinet M et al (eds) *Eddy covariance: a practical guide to measurement and data analysis*. Springer, Dordrecht, pp 59–83
- Shimizu T (2007) Practical applicability of high frequency correction theories to CO₂ flux measured by a closed-path system. *Boundary-Layer Meteorol* 122:417–438
- Shimizu T, Suzuki M, Shimizu A (1999) Examination of a correction procedure for the flow attenuation in orthogonal sonic anemometers. *Boundary-Layer Meteorol* 93:227–236
- Shimizu T, Kumagai T, Kobayashi M, Tamai K, Iida S, Kabeya N, Ikawa R, Tateishi M, Miyazawa Y, Shimizu A (2015) Estimation of annual forest evapotranspiration from a coniferous plantation watershed in Japan (2): comparison of eddy covariance, water budget and sap-flow plus interception loss. *J Hydrol* 522:250–264
- Siebicke L, Hunner M, Foken T (2012) Aspects of CO₂-advection measurements. *Theor Appl Climatol* 109:109–131

- Su H-B, Schmid HP, Grimmond CSB, Vogel CS, Oliphant AJ (2004) Spectral characteristics and correction of long-term eddy-covariance measurements over two mixed hardwood forests in non-flat terrain. *Boundary-Layer Meteorol* 110:213–253
- Sun J (2007) Tilt corrections over complex terrain and their implication for CO₂ transport. *Boundary-Layer Meteorol* 124:143–159
- Thomas C, Foken T (2002) Re-evaluation of integral turbulence characteristics and their parameterizations. In: 15th conference on turbulence and boundary layers. American Meteorological Society, Boston, pp 129–132
- Turnipseed AA, Anderson DE, Blanken PD, Baugh WM, Monson RK (2003) Airflows and turbulent flux measurements in mountainous terrain. Part I. Canopy and local effects. *Agric For Meteorol* 119:1–21
- Vickers D, Mahrt L (2006) Contrasting mean vertical motion from tilt correction methods and mass continuity. *Agric For Meteorol* 138:93–103
- Webb EK, Pearman GI, Leuning R (1980) Correction of flux measurements for density effects due to heat and water vapour transfer. *Q J R Meteorol Soc* 106:85–100
- Wieser A, Fiedler F, Corsmeier U (2001) The influence of the sensor design on wind measurements with sonic anemometer systems. *J Atmos Ocean Technol* 18:1585–1608
- Wilczak JM, Oncley SP, Stage SA (2001) Sonic anemometer tilt correction algorithms. *Boundary-Layer Meteorol* 99:127–150
- Yuan R, Kang M, Park S, Hong J, Lee D, Kim J (2007) The effect of coordinate rotation on the eddy covariance flux estimation in a hilly Koflux forest site. *Korean J Agric For Meteorol* 9:100–108
- Yuan R, Kang M, Park S, Hong J, Lee D, Kim J (2011) Expansion of the planar-fit method to estimate flux over complex terrain. *Meteorol Atmos Phys* 110:123–133